Developmental Cell
Short Article

Target-Mediated Protection of Endogenous MicroRNAs in *C. elegans*

Saibal Chatterjee,[1] Monika Fasler,[1] Ingo Büssing,[1] and Helge Großhans[1,*]
[1]Friedrich Miescher Institute for Biomedical Research, P.O. Box 2543, CH-4002 Basel, Switzerland
*Correspondence: helge.grosshans@fmi.ch
DOI 10.1016/j.devcel.2011.02.008

SUMMARY

MicroRNAs (miRNAs) are tightly regulated through transcriptional and posttranscriptional mechanisms, including degradation by nucleases. Here, we report that in *C. elegans*, target mRNAs can protect their cognate miRNAs from degradation in vivo. We show that the *let-7(n2853)* mutation destabilizes the mature *let-7* miRNA by impairing this protection. Moreover, presence of a cognate target or depletion of the *xrn-1* (XRN1) or *xrn-2* (XRN2/Rat1p) exoribonucleases enforces accumulation of certain miRNA passenger (miR*) strands. Thus, following biased miRNA strand loading into Argonaute, elimination of nonfunctional RNAs can further refine miRNA strand selection. Conversely, by aligning the levels of miRNAs with those of their targets, the opposing activities of mature miRNA degradation and target-mediated miRNA protection (TMMP) may enable dynamic expression of either mature strand of a pre-miRNA, and evolution of miRNAs. Thus, it seems that mRNAs are more than inert targets and function with miRNAs in a network of mutual regulation.

INTRODUCTION

MicroRNAs (miRNAs) are endogenous noncoding RNAs that posttranscriptionally modulate expression of mRNAs, collectively regulating diverse developmental and physiological processes (Bushati and Cohen, 2007). Following transcription of the primary miRNA, processing by the ribonuclease (RNase) Drosha yields an ~65 nucleotide (nt) long pre-miRNA (Carthew and Sontheimer, 2009). In the cytoplasm, cleavage of the pre-miRNA by the RNase Dicer generates an ~22 nt long miRNA guide:passenger (miR:miR*) duplex, which is loaded onto an Argonaute protein (AGO; ALG-1 and ALG-2 in *C. elegans*) to form a pre-miRISC complex (*miR*NA-*I*nduced *S*ilencing *C*omplex). Subsequent removal of the miR* and AGO "programming" with the miR strand leads to the generation of an active miRISC that can silence partially complementary target mRNAs through translational repression, deadenylation, and/or mRNA degradation (Carthew and Sontheimer, 2009). Strand selection is thought to be largely "hard-wired," i.e., determined by thermodynamic asymmetry of the ends of the miR:miR* duplex further refined by preferences for specific 5′ nucleotide and structural features in the pre-miRNA. However, unknown parameters may occasionally override these hard-wired preferences (Okamura et al., 2008).

We have recently shown that miRNAs are subject to degradation by the 5′→3′ exoribonuclease XRN-2 both in vitro and in vivo (Chatterjee and Großhans, 2009). In vitro, this process involved miRNA release from AGO, followed by degradation by XRN-2, and both release and degradation were prevented when mRNA was present that had binding sites for the miRNA.

To investigate whether such protection also occurs in vivo, we have expressed here targets of miRNAs that normally accumulate little and demonstrate that this increases levels of the cognate miRNAs in *C. elegans*. Conversely, decreasing the availability of endogenous targets reduces mature miRNA levels. Notably, expression of a target mRNA, or depletion of *xrn-2* or its paralogue *xrn-1*, can also force the accumulation of certain miR* passenger strands. This suggests that discrimination between miR and miR* can, for some miRNAs, occur after incorporation into AGO and independently of thermodynamic asymmetry of duplex ends. It highlights a mechanism whereby, depending on target availability, new miRNAs can be generated from existing loci, and whereby miR:miR* ratios may be altered during the course of development or in different tissues.

RESULTS

Target Availability Modulates the Levels of the Mature *let-7(n2853)* miRNA

Recently, we have established an in vitro assay in which a pre-miRNA undergoes Dicer-mediated processing followed by programming of AGO with the guide strand (Chatterjee and Großhans, 2009). Pairing with a partially complementary target RNA stabilizes the mature miRNA, whereas mutations in the target site abrogate miRNA protection. Although these data support an attractive model of target-dependent miRNA homeostasis, in which miRNA degradation aligns the levels of programmed AGO with that of its targets, to our knowledge, there has been no in vivo support for this model as yet.

To test the target-mediated miRNA protection (TMMP) model in vivo, we first examined the *let-7(n2853)* miRNA, which differs from its wild-type counterpart by a single point mutation in the "seed" (Reinhart et al., 2000). As for wild-type *let-7* (Chatterjee and Großhans, 2009), TMMP acts on *let-7(n2853)* in vitro: when we incubated in vitro-transcribed, radiolabeled pre-*let-7(n2853)* with *C. elegans* lysate, it was turned over rapidly, and mature *let-7(n2853)* miRNA accumulated only when an in vitro-transcribed target mRNA was supplied (Figure 1A). The target consisted of the *Renilla* luciferase (*RL*) coding region and a 3′

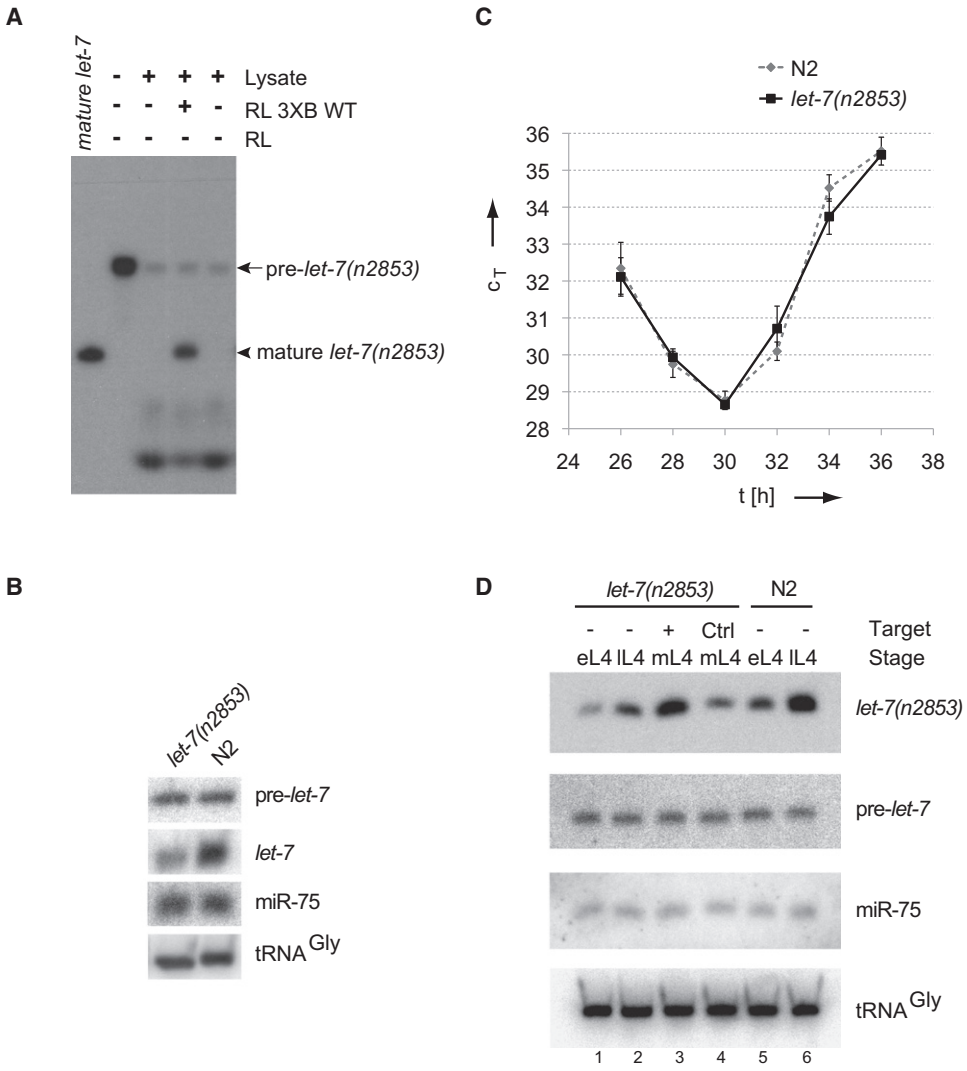

Figure 1. Presence of a Target mRNA Stabilizes the *let-7(n2853)* miRNA In Vitro and In Vivo

(A) A radiolabeled pre-*let-7* miRNA (arrow) carrying the *n2853* mutation was incubated with or without *C. elegans* larval lysate and an in vitro-transcribed target mRNA ("RL 3XB WT"; carrying three bulged *let-7(n2853)* binding sites) or an mRNA lacking target sites ("RL"). Radiolabeled mature *let-7* is loaded as a reference. [B]) Northern blot analysis on total RNA from mid-L4 stage *let-7(n2853)* mutant and wild-type (N2) animals was used to detect the indicated RNAs. Pre-*let-7* and mature *let-7* signal are from the same autoradiograph, but images were processed separately to avoid saturation of mature *let-7* signal when adjusting levels for the weaker pre-*let-7* signal. (C) RT-qPCR analysis of pri-*let-7* levels in *let-7(n2853)* mutant and N2 animals during the L4 stage. Symbols indicate the mean threshold cycle (c_T) values derived from two biological replicates, error bars the individual measurements; values were normalized to expression of the *ama-1* control gene. Time is in hours of postembryonic development at 25°C.D) Northern blot analysis of total RNA from N2 and *let-7(n2853)* animals using the indicated probes. *let-7(n2853)* animals expressed no target transgene (lanes 1 and 2), a *let-7(n2853)* target (lane 3), or a control target (lane 4; containing *miR-241*mut* sites). N2 animals expressed no target transgene. As transgenic animals grew slightly asynchronously and were mixed L4 (mL4) stage, both early and late L4 (eL4 and lL4) stage animals were used as nontransgenic controls. $tRNA^{Gly}$ is the loading control in (B) and (D).

untranslated region (3′UTR) with three miRNA complementary sites containing a central 5 nt bulge, analogous to a functional *let-7* target (Pillai et al., 2005).

Although pre-*let-7(n2853)* is thus processed efficiently in vitro, levels of mature *let-7(n2853)* are substantially reduced in vivo relative to wild-type *let-7* (Reinhart et al., 2000; see below). Despite the widespread use of the *n2853* allele in studies of *let-7* as a developmental regulator and model miRNA, the cause has remained unknown. We speculated that impaired target binding due to the seed mutation might make the miRNA susceptible to degradation, which would suggest that pre-*let-7* and pri-*let-7* levels should be comparable in *let-7(n2853)* mutant and wild-type animals. This is indeed what we found (Figures 1B and 1C; Hurschler et al., 2011).

To determine directly whether the presence of a target could rescue reduced *let-7(n2853)* levels in vivo, we expressed the *let-7(n2853)* target, fused to *gfp*, from a ubiquitous *tbb-1* promoter. Following extraction of total RNA, miRNA levels were probed by northern blotting. Although target mRNA expression occurred from an extrachromosomal array, which is stochastically

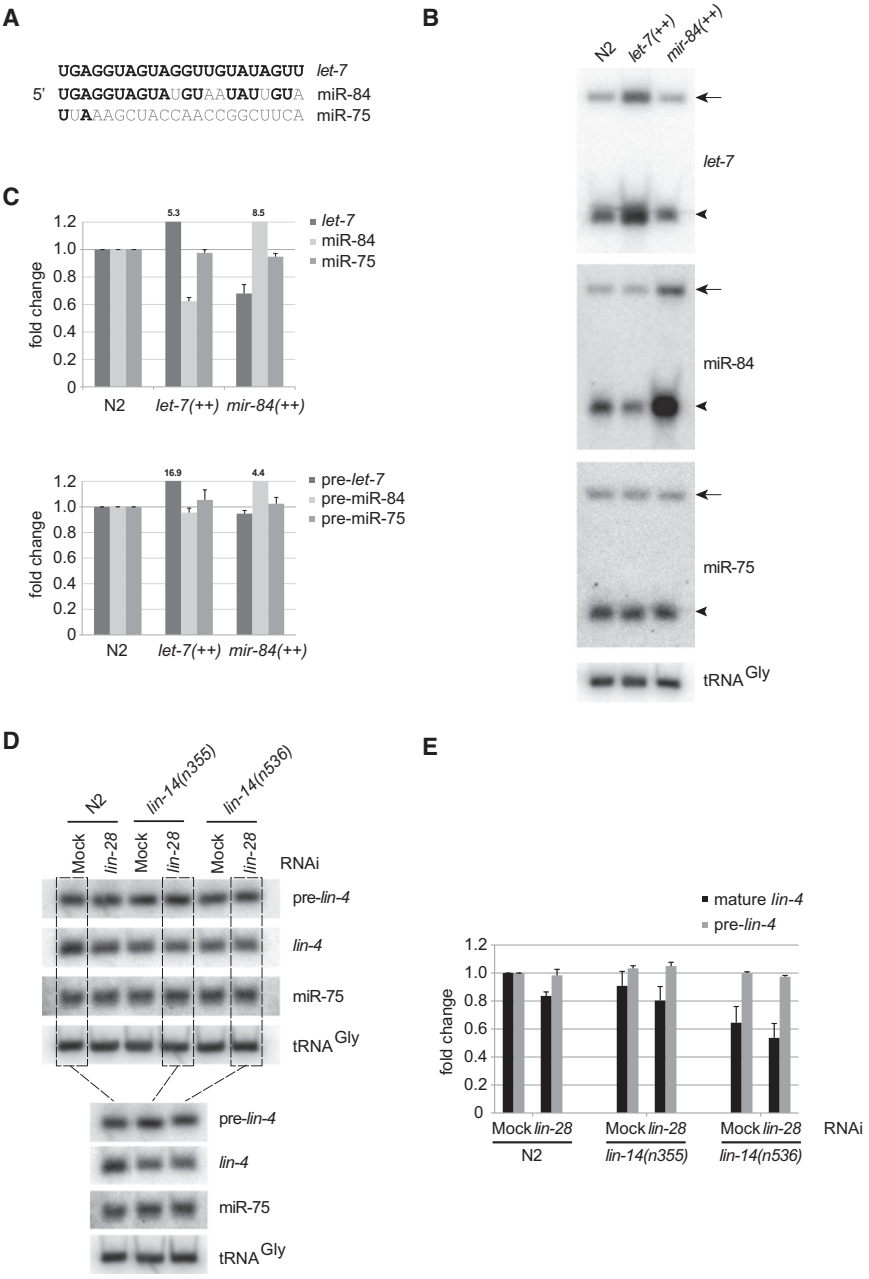

Figure 2. Reduced Availability of Endogenous Targets Reduces Mature miRNA Levels

(A) Sequence comparison of *let-7*, miR-84, and miR-75; identical nucleotides are shown in bold black.B) Northern blotting on total RNA from N2, *let-7* overexpressing (*let-7(++)*), and *mir-84* overexpressing (*mir-84(++)*) animals was used to detect the indicated mature miRNAs and their precursors.C) Fold changes (mean + SEM; normalized to $tRNA^{Gly}$ for loading) relative to N2 for experiments described in (B) with n = 5 biological replicates. Insufficient RNA amounts prevented detection of pre-miRNAs in some experiments such that n = 4 for pre-*let-7* and n = 2 for pre-miR-84 and pre-miR-75. Bars are truncated at 1.2 for clarity; values in excess are indicated.D) Northern blotting on total RNA from L2-stage N2, *lin-14(n355)*, and *lin-14(n536)* animals exposed to mock RNAi or RNAi against a second *lin-4* miRNA target, *lin-28*. The *lin-14* mutations delete *lin-4* binding sites in the *lin-14* 3′UTR. Correct staging was confirmed by counting of germ cell nuclei. To permit direct comparison of RNA levels in wild-type animals and *lin-14; lin-28* double mutants, a spliced autoradiograph is also included. Mock RNAi in this and all subsequent figures uses the empty feeding RNAi vector L4440.E) Fold changes (mean + SEM; normalized to $tRNA^{Gly}$ for loading) relative to N2 on mock RNAi for experiments described in (D) with six biological replicates (three for pre-*lin-4*).

lost during cell mitosis and, thus, not present in all cells, we found that mature *let-7(n2853)* amounts increased to levels approaching that of its wild-type counterpart (Figure 1D). Notably, pre-*let-7(n2853)* levels remained unaffected. Moreover, a transgene containing an irrelevant target sequence did not affect mature *let-7(n2853)* levels. Thus, TMMP can occur in vivo. Furthermore, our findings collectively suggest that partial loss of TMMP is a likely cause for reduced in vivo accumulation of *let-7(n2853)*.

Reduced Availability of Endogenous Targets Decreases Cognate miRNA Accumulation

To test the TMMP model without an artificial target, and for wild-type miRNAs, we studied the competition between miR-84 and *let-7*. These miRNAs are similar in sequence (Figure 2A) and share an overlapping target set (Resnick et al., 2010), and the TMMP model predicts that overexpressing one could decrease levels of the other through competition for shared targets. Indeed, although their expression patterns and targets overlap only partially, overexpression of *let-7* decreased miR-84 levels, whereas overexpression of *mir-84* decreased *let-7* levels (Figures 2B and 2C). By contrast the levels of an unrelated miRNA, miR-75, changed little. Moreover, changes occurred downstream of the pre-miRNAs, whose levels were equally unchanged. These findings validate a prediction of the TMMP model.

The most direct way to test TMMP as a physiological event is by modulating the levels of endogenous targets, but miRNAs tend to have many targets, whose identities are frequently not known, and which cannot be co-depleted efficiently. However, the *lin-4* miRNA allowed us to study the effect of simultaneous depletion of two validated targets, *lin-14* and *lin-28* (Moss et al., 1997; Wightman et al., 1993). We combined RNAi-mediated depletion of *lin-28* with the *lin-14(n355)* or the *lin-14(n536)* mutant allele, respectively. *lin-14(n355)* harbors an inversion or insertion of at least 10 kb of unknown DNA sequence such that ~1300 nt of *lin-14* 3′UTR, including all seven putative *lin-4*

binding sites, are replaced by ~300 nt of unknown sequence (Wightman et al., 1991). *lin-14(n536)* harbors a well-defined internal 3′UTR deletion removing five of the binding sites (Wightman et al., 1991). Strikingly, despite the likely presence of many additional *lin-4* targets, either combination of *lin-14* and *lin-28* mutations was sufficient to reduce *lin-4* levels (Figures 2D and 2E). By contrast, pre-*lin-4* levels remained unaffected. The unknown RNA sequence added to the *lin-14(n355)* 3′UTR might explain that the effects were more robust for *lin-14(n536)* than *lin-14(n355)*. We conclude that endogenous target mRNAs can exert TMMP on endogenous miRNAs.

Target Availability Promotes miRISC Residency of a miRNA Passenger Strand (miR*)

According to a widely accepted model of RISC loading, the strand with the less strongly base paired 5′ end within the miR:miR* duplex is selectively used to program miRISC (Carthew and Sontheimer, 2009). This model was developed in analogy to loading of siRNAs into RISC (Khvorova et al., 2003; Schwarz et al., 2003). However, whereas a mechanism of asymmetry sensing through the Dicer accessory protein R2D2 has been established for siRNA loading in flies (Tomari et al., 2004), comparable mechanistic insight is lacking for miRNA strand selection, and the validity of this model relies largely on bioinformatic and statistical observations (Khvorova et al., 2003; Han et al., 2006). Moreover, because miRNAs exist for which both ends of a putative miR:miR* duplex are either symmetric or the 5′ end of the miR* is even less stably base paired than the 5′ end of the miR (Griffiths-Jones et al., 2007), this model may not be universally valid. The discrepancy prompted us to investigate whether miR* strands could be stabilized by targets.

We first examined pre-*let-7*. As reported (Chatterjee and Großhans, 2009), target RNA against the miR strand stabilized mature *let-7* when pre-*let-7* was processed in the in vitro system (Figure 3A). However, no product of such size was observed when an assay was performed in the presence of an RNA with binding sites for the *let-7** strand (Figure 3A). Because the *let-7* miR:miR* duplex reveals a clear thermodynamic asymmetry (Krüger and Rehmsmeier, 2006) with pairing of the 5′ end of the miR strand much more unstable relative to that of the 5′ end of the miR* strand (Figure 3A), this observation is consistent with thermodynamic strand selection preventing passenger strand loading into AGO and, thus, precluding its target-mediated stabilization.

In contrast to the ''canonical'' miR:miR* duplex observed for *let-7*, the duplex of its sequence-related ''sister'' miR-241 is less thermodynamically stable at the miR* 5′ end than the miR 5′ end (Figure 3B). (Note that deep-sequencing data (Ruby et al., 2006) confirm the annotated 5′ ends of miR-241 and miR-241* [D. Gaidatzis, personal communication].) Hence, we subjected pre-miR-241 to the in vitro TMMP assay. As expected, target RNA against the miR strand could stabilize a mature miR-241-sized strand (Figure 3B). However, unlike for *let-7**, an assay performed in the presence of a mRNA with miR-241* target sites also yielded a band around the size of the miR*. Mutations disrupting the seed match of the target to miR-241* greatly diminished this accumulation. We confirmed the identities of the bands by northern blot analysis on the products of an assay using cold pre-miR-241 as a substrate (Figure 3C).

Of note, when examined in the presence of their respective target mRNAs, miR-241 was more abundant than miR-241*, as revealed by comparing the respective signal intensities for mature miRNA and untreated pre-miRNA (Figure 3C; compare lanes 2 and 4 in upper panel, and lanes 2 and 5 in lower panel, respectively). (Although miR-241* appears more abundant in Figure 3B, this is an artifact of its being more U-rich than miR-241 and, thus, containing more radiolabel per molecule.) This suggests preferential RISC loading of the miR strand. Additional elements beyond thermodynamic asymmetry, perhaps the identity of the 5′-terminal nucleotide (Czech et al., 2009; Ghildiyal et al., 2010; Okamura et al., 2009), may thus bias strand incorporation.

In *Drosophila*, both miR and miR* strands are retained for some miRNAs. However, typically only the miR strand is incorporated into the miRISC Argonaute AGO1, whereas the miR* strand is loaded into AGO2, the siRNA-specific AGO (Czech et al., 2009; Ghildiyal et al., 2010; Okamura et al., 2009). To confirm that miR-241* was loaded into the miRISC AGOs ALG-1/-2, we performed the pre-miR-241 processing assay with lysate from a strain in which ALG-1 and ALG-2 were fused to GFP (Figure 3D, upper panel), followed by immunoprecipitation using an anti-GFP antibody. In the presence of a target RNA for the miR* strand, we could specifically coprecipitate miR-241* (Figure 3D, middle panel). Depletion of miR-241* from the supernatant suggests that it is indeed predominantly associated with ALG-1/-2 (Figure 3D, lower panel). Thus, the target stabilizes ALG-1/-2-associated miR-241*.

Selective Stabilization of miR-241* Upon In Vivo Expression of a Target mRNA

Although the miR-241* strand could be stabilized by TMMP in vitro, it is rare in vivo (Ruby et al., 2006; Kato et al., 2009). Thus, to rule out that target RNA-stabilized miR-241* incorporated fortuitously into ALG-1/-2 under in vitro conditions, we sought to validate our observations in vivo. To this end we generated worms that expressed a miR-241* target transgene from the *tbb-1* promoter. Northern blotting on total RNA from this strain detected considerable accumulation of miR-241* relative to a nontransgenic control (Figure 4A). Moreover, a mutant miR-241* target, containing a disrupted match to the miR-241* seed, failed to stabilize miR-241* efficiently. Hence, the mechanistic insights into RISC loading of mature miR/miR* strands obtained through our in vitro experiments are also valid in a physiological context, and we can conclude that both in vitro and in vivo target availability can stabilize an AGO-residing strand that would otherwise be degraded.

Depletion of miRNA Turnover Enzymes Affects a Subset of miR* Strands

If unavailability of a target RNA subjects an AGO-residing miRNA strand to degradation, does turnover involve the miRNA-degrading enzyme XRN-2 (Chatterjee and Großhans, 2009)? We tested this possibility by examining miR-241* levels in vivo following *xrn-2(RNAi)* and, indeed, observed increased miR-241* levels (Figure 4B). In contrast to miR-241*, the *let-7** strand did not accumulate (Figure 4B); a finding in agreement with our in vitro TMMP data and consistent with thermodynamic asymmetry as the key determinant in strand selection from pre-*let-7*.

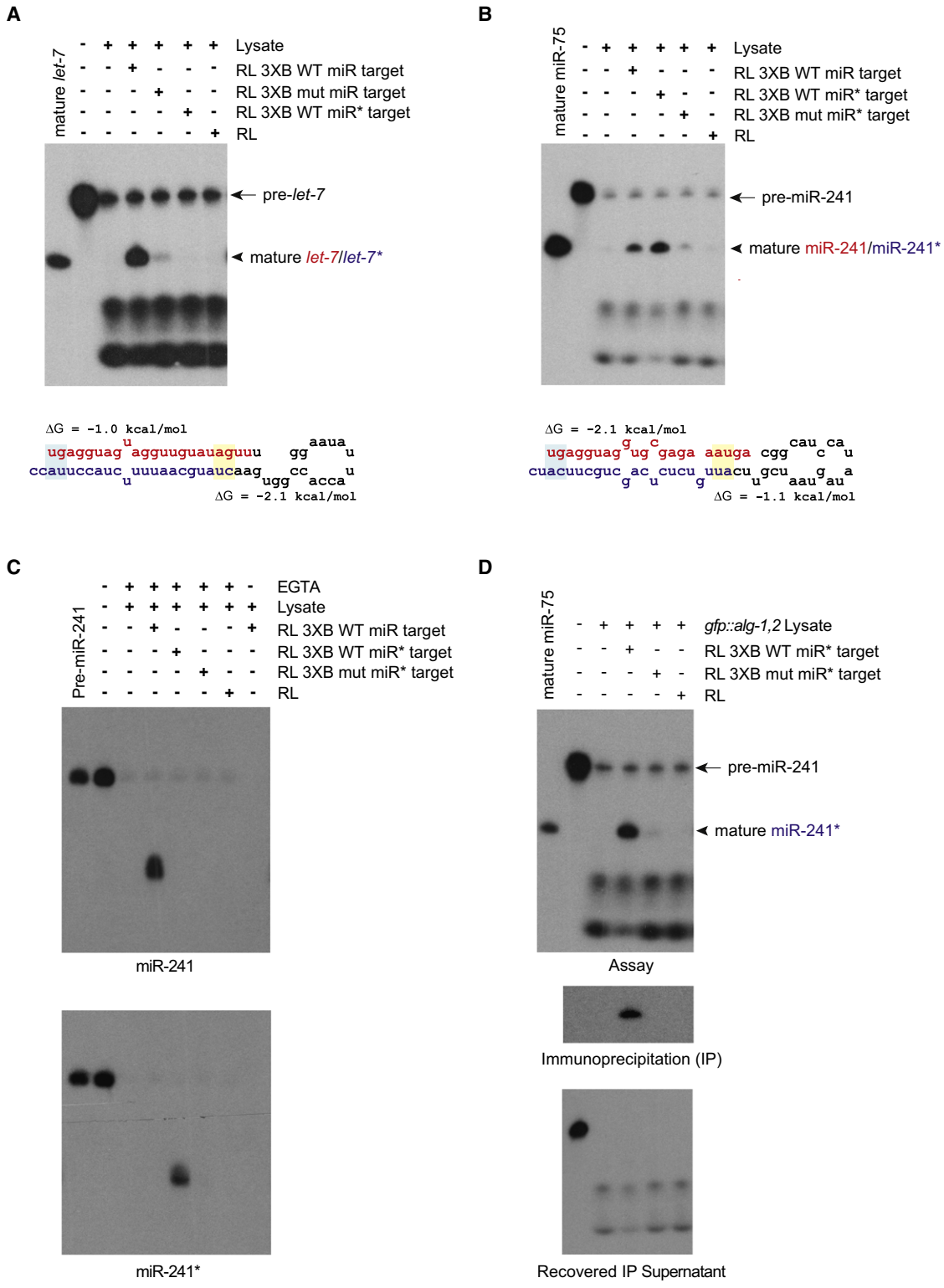

Figure 3. Target Availability Determines RISC Residency of a miR*

(A) In vitro-transcribed, radiolabeled wild-type pre-*let-7* miRNA (arrow) was incubated with or without *C. elegans* larval lysate and mRNAs containing binding sites for the *let-7* guide, mutant variants thereof, or for the *let-7** passenger. Radiolabeled mature *let-7* is a reference in the first lane. In the schematic drawing of the pre-miRNAs, the guide strand is shown in red, the passenger strand in blue. Base pairs involving the 5′-terminal 2 nt of guide and passenger strand are shaded in light blue and yellow, respectively, and the corresponding ΔG values are indicated.B) Experiment as in (A) but using in vitro-transcribed radiolabeled pre-miR-241 as substrate and targets containing binding sites for miR-241, miR-241* or mutated miR-241* sites, mismatched to the seed sequence. Radiolabeled mature

We further examined the levels of miR-58* and miR-73*, two miR* strands that originate from symmetric miR:miR* duplexes (Figure 4C), but where database annotation and deep sequencing data reveal a strong bias toward accumulation of only one, namely the miR strand (Griffiths-Jones et al., 2007; Ruby et al., 2006; Kato et al., 2009). Depletion of *xrn-2* also elevated the levels of these miR* strands (Figure 4C).

In yeast, Xrn1p and Xrn2p (Rat1p) are partially redundant in various RNA-processing pathways (Poole and Stevens, 1995; Petfalski et al., 1998; Henry et al., 1994). Hence, we examined the possibility that XRN-1 is also involved in miR* turnover. Unlike an earlier RNAi construct (Kamath et al., 2003), a vector encompassing the entire *xrn-1* cDNA permitted efficient depletion of XRN-1 (see Figure S1 available online), and this resulted in accumulation of miR-241*, miR-58*, and miR-73*, but not *let-7** (Figures 4B and 4C). Thus, both XRN-1 and XRN-2 mediate miRNA passenger strand degradation. Accumulation of miR-241* but not of *let-7** further suggests that XRN-1/-2-mediated degradation preferentially affects miR* strands that can be loaded onto AGO.

Our newly designed RNAi construct against *xrn-1* also permitted us to reexamine whether XRN-1 was involved in miR strand turnover. Previous experiments had failed to support this notion (Chatterjee and Großhans, 2009) but were done under conditions of inefficient *xrn-1* knockdown (Figure S1A). By contrast, with the more extensive depletion, we now observed accumulation of miR strands in *xrn-1(RNAi)* animals (Figure 4D), supporting a function of XRN-1 also in miRNA guide strand degradation. Interestingly, in humans XRN1, but not XRN2, has been implicated in the turnover of miR-382 (Bail et al., 2010).

TMMP Counteracts miRNA Degradation by XRN-1 and XRN-2

Our findings suggest that TMMP and miRNA degradation by XRN-1/-2 are opposing mechanisms. To test this notion further, we examined how the presence of targets affected the response of miRNAs to depletion of the RNases. Exploiting the fact that TMMP of *let-7(n2853)* is impaired relative to wild-type *let-7* (Figure 1), we compared how *xrn-1(RNAi)* and *xrn-2(RNAi)* affected these miRNAs. Depletion of these RNases resulted in a respective 3.8- and 2.9-fold upregulation of *let-7(n2853)* relative to mock RNAi treatment (Figure 4E). This effect was blunted for wild-type *let-7*, where upregulation did not exceed 1.6-fold. By contrast, changes for an unrelated miRNA, miR-77, were comparable in *let-7* mutant and wild-type animals. These results are consistent with TMMP functioning by opposing XRN-1/-2 activity.

To study the effect in a more defined situation, we exposed animals carrying a transgene with miR-241* target sites or a control 3′UTR to RNAi against *xrn-1* and *xrn-2*, respectively. Again, we found that depletion of the RNases led to a substantial upregulation of miR-241* in the absence of a miR-241* target but had a much-reduced effect in its presence (Figure 4F). By contrast, miR-241 upregulation occurred equally efficiently in both transgenic strains, and pre-miR-241 levels were comparable under all conditions. We conclude that TMMP acts indeed in opposition to miRNA degradation mediated by XRN-1 and XRN-2.

DISCUSSION

We have previously identified a miRNA turnover pathway involving XRN-2 (Chatterjee and Großhans, 2009), but it had remained unclear whether the TMMP that we observed in vitro also held true in vivo. We now show this to be so, providing direct support for the notion that the opposing activities of mature miRNA degradation and TMMP can serve to align the levels of programmed AGO with that of its targets. By confirming this for the mutant *let-7(n2853)* miRNA, we also resolve a long-standing mystery, namely, why a mutation in the seed of this miRNA decreases its abundance (Reinhart et al., 2000; Chatterjee and Großhans, 2009): our data indicate that this is because impaired target binding diminishes the protection of *let-7 (n2853)* RNA from degradation. Whether the protection occurs through simple competition between target binding and miRNA degradation, or through altered localization or modification of target-bound miRISC remains to be addressed. Clearly, the latter would be an attractive option in that even substoichiometric target mRNA amount might suffice for substantial miRNA protection, if the modification were to persist for some time even after the target has been released or degraded.

Our finding that a target can stabilize a miR* strand both in vitro and in vivo has two major implications. First, it suggests that TMMP provides a possible way of evolutionary diversification of miRNAs from existing loci, by driving accumulation of previously unused passenger strands once targets, and thus potential biological functions, have been acquired. Intriguingly, both in nematodes and Drosophilids, a number of members of miRNA families appear to have undergone ‘‘arm switching’’ (de Wit et al., 2009; Okamura et al., 2008), i.e., miR* to miR transition, and it is tempting to speculate that this might also be occurring for the *C. elegans* miR-241. Although ‘‘unused’’ miR* strands of preexisting pre-miRNAs, particularly those of extended miRNA families, are an obvious target for TMMP-driven diversification of miRNAs, any other hairpin that is processed by Dicer and loaded into Argonaute could conceivably be subject to this process. Conversely, for miR* strands (or other miRNA-like small RNAs) lacking targets, the turnover machinery may play a surveillance role to clear out idle RNAs from AGO, promoting formation of active RISC containing miRNAs with targets. Therefore, mature miRNA turnover and TMMP together serve to maintain the robustness of the existing genetic makeup by constituting another layer of RISC regulation.

Second, selection of functional miRNAs, with targets, through mature miRNA degradation and TMMP, may not only be relevant to de novo evolution of miRNAs, or demise of existing ones, but also introduce a new dynamic to spatial and temporal miRNA expression patterns. For instance it was noticed for some miRNAs that the ratio of miR to miR* changed during *Drosophila*

miR-75 serves as size reference.C) Experiment as in (B) but using cold pre-miR-241 as substrate and lysates pretreated with micrococcal nuclease (MN) to remove all endogenous RNA. MN activity is terminated by EGTA treatment; omission of this step (rightmost lane) prevents miRNA accumulation. Product detection occurs by northern blot analysis.D) Pre-miR-241 turnover assay using target mRNAs as indicated and lysates from animals expressing *gfp::alg-1, gfp::alg-2* (‘‘GFP/AGO’’). Mature miR-241* passenger accumulates in the presence of a cognate target (top) and coimmunoprecipitates with GFP/AGO (middle), whereas it is depleted from the supernatant (bottom).

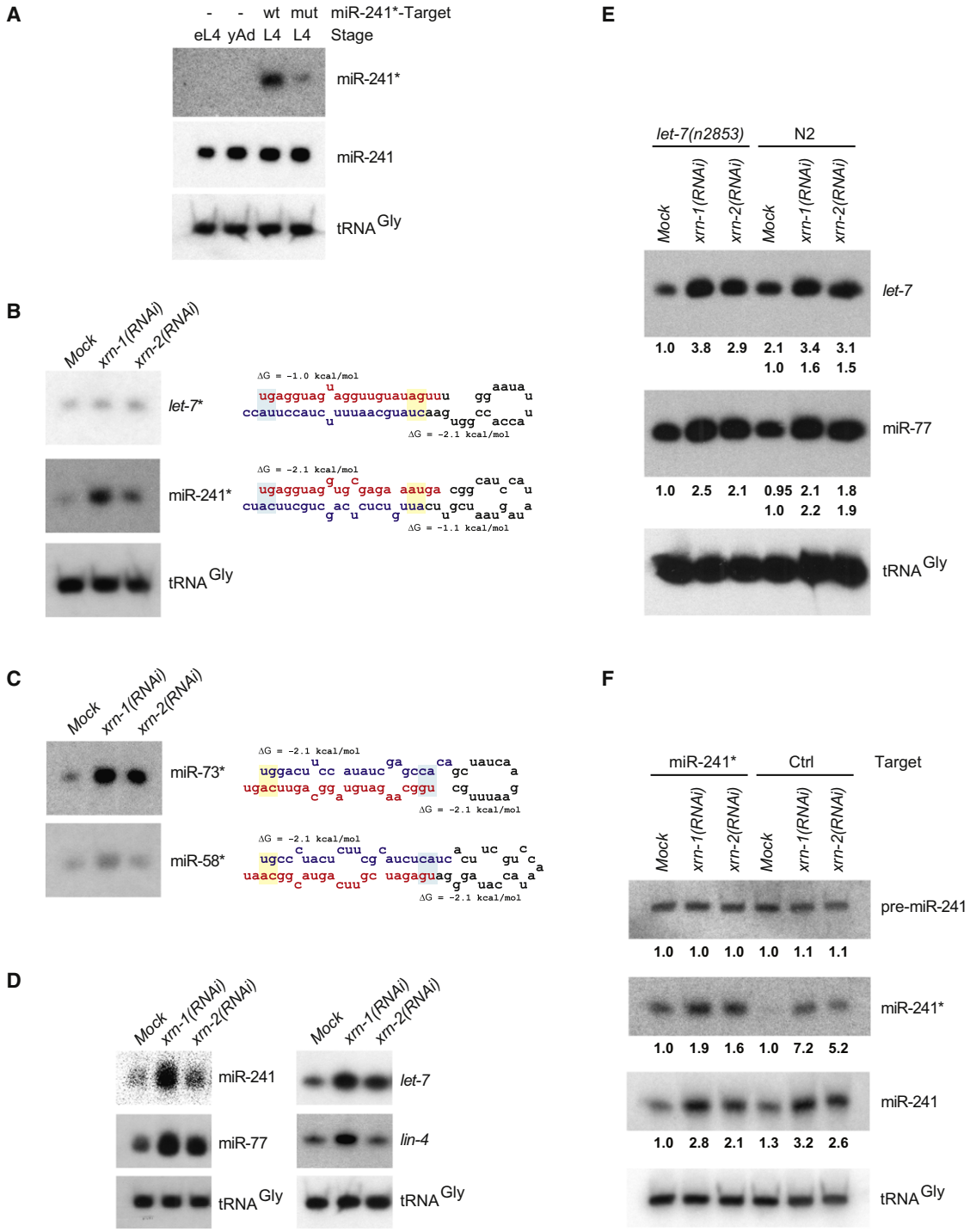

Figure 4. Target Availability and Turnover Machinery Together Govern RISC Residency In Vivo

(A) Northern blot analysis of total RNA from N2 animals expressing no, a wild-type or a mutant (seed-mismatched) miR-241* target transgene. As transgenic animals grew slightly asynchronously and were mixed L4 stage, we included both early L4 (eL4) and young adult (yAd) nontransgenic animals as controls.B–D) Northern blot analysis of total RNA from (B), (C) RNAi-enhanced *rrf-3* or (D) N2 wild-type animals exposed to the indicated RNAi. The same membrane was used for (B) and (C); the loading control $tRNA^{Gly}$ is shown in (B).E) Northern blot analysis of total RNA from N2 and *let-7(n2853)* animals exposed to RNAi as indicated. Numbers represent fold changes relative to *let-7(n2853)* on mock RNAi (upper rows) and N2 on mock RNAi (lower rows), respectively, following normalization to $tRNA^{Gly}$ for loading.F) Northern blot analysis of total RNA from N2 animals with a miR-241* target transgene or a control transgene containing the nontargeted *unc-54* 3′UTR ("Ctrl") exposed to RNAi as indicated. Numbers represent fold changes of pre-miR-241, miR-241, and miR-241*, respectively, relative to the respective mock RNAi treatment after normalization to $tRNA^{Gly}$. Pre-miR-241 was detected using the probe against miR-241. See also Figure S1.

development (Okamura et al., 2008), as well as in mice (Chiang et al., 2010). Our results reveal a possible mechanism to achieve such dynamics.

Our findings also have implications for current models of strand selection from the miR:miR* duplex. For siRNAs, strand selection is a result of differential loading into RISC, guided by thermodynamic asymmetry of the duplex ends (Khvorova et al., 2003; Schwarz et al., 2003; Tomari et al., 2004). Although this model is generally thought to apply to miRNAs as well (Carthew and Sontheimer, 2009), direct experimental support that strand selection occurs during miRISC loading has been missing. Although our experiments were not designed to examine AGO loading directly, our results illustrate two possible modes of strand selection. A *let-7:let-7** duplex conforms to the notion of strand selection based on thermodynamic asymmetry, and, consistent with the idea that strand fate is decided during loading, no accumulation of *let-7** can be forced through addition of a *let-7** target mRNA. Thus, it appears that little or no single-stranded *let-7** associates with AGO. By contrast, for miR-241:miR-241*, accumulation of miR-241* within AGO can be forced by supplying a target, demonstrating that single-stranded miR-241* can be loaded into AGO. In this case, miRNA strand selection is not fully determined during loading but is scrutinized and nullified by a "proof-reading" mechanism that eliminates target-less miRNAs while legitimizing utile, i.e., target-bound, miRNAs for RISC residency. The fact that depletion of *xrn-1* and/or *xrn-2* causes accumulation of miRNA passenger strands from the miRNAs lacking the canonical miR:miR* asymmetry such as miR-241, but not of miRNAs exhibiting such asymmetry (e.g., *let-7*), then suggests that these two RNases preferentially act on miRNAs that transit through AGO, as opposed to free small RNAs. How such a preference is achieved remains to be established, although specific recruitment of the RNases to AGO is a tempting speculation.

In sum we advocate a post-loading proofreading mechanism that refines and diversifies RISC programming. The fact that thermodynamic asymmetry appears underdeveloped in *C. elegans* (de Wit et al., 2009) suggests that the mechanism may apply more widely. It will be particularly interesting to learn to which extent post-loading miRNA strand selection mechanisms can contribute to the recently observed dynamic changes in miR:miR* ratios.

Finally, we note that it was recently reported that specific miRNA target site architectures, distinct from the one we used here, can induce cognate miRNA degradation in *Drosophila* and human cells (Cazalla et al., 2010; Ameres et al., 2010). It remains to be established whether this process also operates in *C. elegans* and, conversely, whether TMMP is active in other animals. However, collectively, these data suggest the exciting possibility that rather than being inert targets of miRNAs, mRNAs might form a highly dynamic network of mutual regulation with their cognate miRNAs (Seitz, 2009).

EXPERIMENTAL PROCEDURES

Worm Strains, Transgenesis, and RNAi

We used the N2 *C. elegans* var. Bristol wild-type and the following mutant strains: *let-7(n2853)* (Reinhart et al., 2000), MT355: *lin-14(n355)*, MT1149: *lin-14(n536)* (Wightman et al., 1991). We used strains expressing the following transgenes: *gfp::alg-1, gfp::alg-2* (Hutvagner et al., 2004); CT19: *zaIs3[let-7(+), myo-3::gfp]* (Weidhaas et al., 2007); and GR1428: *mgIs45[mir-84++, tub-1::gfp]I* (Hayes et al., 2006). Strains generated for this study (as detailed in the Supplemental Experimental Procedures) were HW628: *unc-119(ed3); xeEx251 [tbb-1::gfp::3xlet-7(n2853)binding sites, myo-2::mCherry, unc-119+]*, HW633: *unc-119(ed3); xeEx256[tbb-1::gfp::3xmir241*binding sites, myo-2::mCherry, unc-119+]*, HW639: *unc-119(ed3); xeEx262[tbb-1::gfp::3xmir241*mut binding sites, myo-2::mCherry, unc-119+]*, HW743: *let-7(n2853); xeEx251* HW744: *let-7(n2853); xeEx262* and HW745: *unc-119(ed3); xeEx268[tbb-1::gfp::unc-54 unc-119+]*. RNAi was performed by feeding on 10 cm plates at 25°C as described (Ding et al., 2008; Großhans et al., 2005). Synchronized L4-stage animals were used unless indicated otherwise with correct staging confirmed by gonad inspection using Nomarski microscopy.

RNA Isolation, Northern Blotting, RT-qPCR

Total RNA isolation, northern blotting, and RT-qPCR were done as described (Chatterjee and Großhans, 2009). Following incubation of RNAs in the lysates, the samples were phenol-chloroform extracted and alcohol precipitated, and subjected to northern probing. To account for the dynamic expression of pri-*let-7* (Büssing et al., 2010), we performed a time course experiment using synchronized N2 grown at 25°C and harvested at 2-hr time intervals during the L4 stage, between 26 and 36 hr. *let-7(n2853)* animals were age matched by gonad inspection to account for a minor developmental delay. Primer sequences are provided in the Supplemental Experimental Procedures.

Preparation of RNA Substrates and Worm Lysates

Pre-miRNAs and 5′-7-methyl-G-capped reporter mRNAs were prepared as described (Chatterjee and Großhans, 2009). The constructs harboring 3X bulged *miR-241/mir-241*//let-7(n2853)/let-7** target sites were prepared by swapping the bulged *let-7* complementary sites in the 3′UTR of pRL 3XB WT vector (Chatterjee and Großhans, 2009) with bulged 3X *miR-241/mir-241*/let-7(n2853)/let-7** complementary sites; relevant sequences of primers are provided in the Supplemental Experimental Procedures. Cleared worm lysates for RNA turnover experiments were prepared as described (Chatterjee and Großhans, 2009).

Target-Mediated miR/miR* Stabilization Assay

Labeled pre-miRNAs (approximately 1 fmol) were incubated with cleared worm lysate (2–10 μg) in 1× assay buffer (Chatterjee and Großhans, 2009) in the absence or presence of 20 fmol of the respective target mRNA in volumes of 10–20 μl at 37°C for 15 min. The reactions were stopped by addition of 1 vol formamide gel loading buffer (Chatterjee and Großhans, 2009), followed by heating at 65°C for 5 min. Equal volumes of the samples were subjected to 7 M urea/8%–12% PAGE, followed by gel drying and autoradiography or phosphor-imaging. Coupled pre-miRNA processing and AGO immunoprecipitation were done as described (Chatterjee and Großhans, 2009).

Image Acquisition and Processing

For quantification of radioactive signals, data acquired with a Storage Phosphor Screen and a Typhoon 9400 scanner were analyzed with ImageQuant TL software (all GE Healthcare). After conversion to TIFF format, Adobe Photoshop software was used to crop images and adjust levels, leaving gamma unaltered.

SUPPLEMENTAL INFORMATION

Supplemental Information includes Supplemental Experimental Procedures and one figure and can be found with this article online at doi:10.1016/j.devcel.2011.02.008.

ACKNOWLEDGMENTS

We thank Benjamin Hurschler for pointing out unchanged pre-*let-7* levels; Dr. Dimos Gaidatzis for bioinformatic analyses; Dr. Witold Filipowicz for critical reading of the manuscript; Dr. Gary Ruvkun and the Caenorhabditis Genetics Center (CGC) for *C. elegans* strains; and Dr. Sarah Newbury for generously sharing an α-XRN-1 antibody. This work was funded by a European Research Council Starting Independent Investigator Award (miRTurn; ERC 2419845), the

Swiss National Science Foundation (SNF 31003A_127052), and FMI, part of the Novartis Research Foundation. S.C. was supported by Marie Curie and EMBO long-term postdoctoral fellowships.

Received: June 28, 2010
Revised: February 14, 2011
Accepted: February 22, 2011
Published: March 14, 2011

REFERENCES

Ameres, S.L., Horwich, M.D., Hung, J.H., Xu, J., Ghildiyal, M., Weng, Z., and Zamore, P.D. (2010). Target RNA-directed trimming and tailing of small silencing RNAs. Science *328*, 1534–1539.

Bail, S., Swerdel, M., Liu, H., Jiao, X., Goff, L.A., Hart, R.P., and Kiledjian, M. (2010). Differential regulation of microRNA stability. RNA *16*, 1032–1039.

Bushati, N., and Cohen, S.M. (2007). microRNA functions. Annu. Rev. Cell Dev. Biol. *23*, 175–205.

Büssing, I., Yang, J.S., Lai, E.C., and Großhans, H. (2010). The nuclear export receptor XPO-1 supports primary miRNA processing in *C. elegans* and *Drosophila*. EMBO J. *29*, 1830–1839.

Carthew, R.W., and Sontheimer, E.J. (2009). Origins and mechanisms of miRNAs and siRNAs. Cell *136*, 642–655.

Cazalla, D., Yario, T., and Steitz, J. (2010). Down-regulation of a host microRNA by a Herpesvirus saimiri noncoding RNA. Science *328*, 1563–1566.

Chatterjee, S., and Großhans, H. (2009). Active turnover modulates mature microRNA activity in *Caenorhabditis elegans*. Nature *461*, 546–549.

Chiang, H.R., Schoenfeld, L.W., Ruby, J.G., Auyeung, V.C., Spies, N., Baek, D., Johnston, W.K., Russ, C., Luo, S., Babiarz, J.E., et al. (2010). Mammalian microRNAs: experimental evaluation of novel and previously annotated genes. Genes Dev. *24*, 992–1009.

Czech, B., Zhou, R., Erlich, Y., Brennecke, J., Binari, R., Villalta, C., Gordon, A., Perrimon, N., and Hannon, G.J. (2009). Hierarchical rules for Argonaute loading in *Drosophila*. Mol. Cell *36*, 445–456.

de Wit, E., Linsen, S.E., Cuppen, E., and Berezikov, E. (2009). Repertoire and evolution of miRNA genes in four divergent nematode species. Genome Res. *19*, 2064–2074.

Ding, X.C., Slack, F.J., and Großhans, H. (2008). The let-7 microRNA interfaces extensively with the translation machinery to regulate cell differentiation. Cell Cycle *7*, 3083–3090.

Ghildiyal, M., Xu, J., Seitz, H., Weng, Z., and Zamore, P.D. (2010). Sorting of *Drosophila* small silencing RNAs partitions microRNA* strands into the RNA interference pathway. RNA *16*, 43–56.

Griffiths-Jones, S., Saini, H.K., Dongen, S.V., and Enright, A.J. (2007). miRBase: tools for microRNA genomics. Nucleic Acids Res. *36*, D154–D158.

Großhans, H., Johnson, T., Reinert, K.L., Gerstein, M., and Slack, F.J. (2005). The temporal patterning microRNA let-7 regulates several transcription factors at the larval to adult transition in *C. elegans*. Dev. Cell *8*, 321–330.

Han, J., Lee, Y., Yeom, K.H., Nam, J.W., Heo, I., Rhee, J.K., Sohn, S.Y., Cho, Y., Zhang, B.T., and Kim, V.N. (2006). Molecular basis for the recognition of primary microRNAs by the Drosha-DGCR8 complex. Cell *125*, 887–901.

Hayes, G.D., Frand, A.R., and Ruvkun, G. (2006). The mir-84 and let-7 paralogous microRNA genes of *Caenorhabditis elegans* direct the cessation of molting via the conserved nuclear hormone receptors NHR-23 and NHR-25. Development *133*, 4631–4641.

Henry, Y., Wood, H., Morrissey, J.P., Petfalski, E., Kearsey, S., and Tollervey, D. (1994). The 5′ end of yeast 5.8S rRNA is generated by exonucleases from an upstream cleavage site. EMBO J. *13*, 2452–2463.

Hurschler, B.A., Harris, D.T., and Großhans, H. (2011). The type II poly(A)-binding protein PABP-2 genetically interacts with the *let-7* miRNA and elicits heterochronic phenotypes in *C. elegans*. Nucl. Acids Res., in press.

Hutvagner, G., Simard, M.J., Mello, C.C., and Zamore, P.D. (2004). Sequence-specific inhibition of small RNA function. PLoS Biol. *2*, E98.

Kamath, R.S., Fraser, A.G., Dong, Y., Poulin, G., Durbin, R., Gotta, M., Kanapin, A., Le Bot, N., Moreno, S., Sohrmann, M., et al. (2003). Systematic functional analysis of the *Caenorhabditis elegans* genome using RNAi. Nature *421*, 231–237.

Kato, M., de Lencastre, A., Pincus, Z., and Slack, F.J. (2009). Dynamic expression of small non-coding RNAs, including novel microRNAs and piRNAs/21U-RNAs, during *Caenorhabditis elegans* development. Genome Biol. *10*, R54.

Khvorova, A., Reynolds, A., and Jayasena, S.D. (2003). Functional siRNAs and miRNAs exhibit strand bias. Cell *115*, 209–216.

Krüger, J., and Rehmsmeier, M. (2006). RNAhybrid: microRNA target prediction easy, fast and flexible. Nucleic Acids Res. *34*, W451–W454.

Moss, E.G., Lee, R.C., and Ambros, V. (1997). The cold shock domain protein LIN-28 controls developmental timing in *C. elegans* and is regulated by the lin-4 RNA. Cell *88*, 637–646.

Okamura, K., Liu, N., and Lai, E.C. (2009). Distinct mechanisms for microRNA strand selection by *Drosophila* Argonautes. Mol. Cell *36*, 431–444.

Okamura, K., Phillips, M.D., Tyler, D.M., Duan, H., Chou, Y.T., and Lai, E.C. (2008). The regulatory activity of microRNA(*) species has substantial influence on microRNA and 3′ UTR evolution. Nat. Struct. Mol. Biol. *15*, 354–363.

Petfalski, E., Dandekar, T., Henry, Y., and Tollervey, D. (1998). Processing of the precursors to small nucleolar RNAs and rRNAs requires common components. Mol. Cell. Biol. *18*, 1181–1189.

Pillai, R.S., Bhattacharyya, S.N., Artus, C.G., Zoller, T., Cougot, N., Basyuk, E., Bertrand, E., and Filipowicz, W. (2005). Inhibition of translational initiation by Let-7 microRNA in human cells. Science *309*, 1573–1576.

Poole, T.L., and Stevens, A. (1995). Comparison of features of the RNase activity of 5′-exonuclease-1 and 5′-exonuclease-2 of Saccharomyces cerevisiae. Nucleic Acids Symp. Ser. *33*, 79–81.

Reinhart, B.J., Slack, F.J., Basson, M., Pasquinelli, A.E., Bettinger, J.C., Rougvie, A.E., Horvitz, H.R., and Ruvkun, G. (2000). The 21-nucleotide let-7 RNA regulates developmental timing in *Caenorhabditis elegans*. Nature *403*, 901–906.

Resnick, T.D., McCulloch, K.A., and Rougvie, A.E. (2010). miRNAs give worms the time of their lives: small RNAs and temporal control in *Caenorhabditis elegans*. Dev. Dyn. *239*, 1477–1489.

Ruby, J.G., Jan, C., Player, C., Axtell, M.J., Lee, W., Nusbaum, C., Ge, H., and Bartel, D.P. (2006). Large-scale sequencing reveals 21U-RNAs and additional microRNAs and endogenous siRNAs in *C. elegans*. Cell *127*, 1193–1207.

Schwarz, D.S., Hutvágner, G., Du, T., Xu, Z., Aronin, N., and Zamore, P.D. (2003). Asymmetry in the assembly of the RNAi enzyme complex. Cell *115*, 199–208.

Seitz, H. (2009). Redefining MicroRNA Targets. Curr. Biol. *19*, 870–873.

Tomari, Y., Matranga, C., Haley, B., Martinez, N., and Zamore, P.D. (2004). A protein sensor for siRNA asymmetry. Science *306*, 1377–1380.

Weidhaas, J.B., Babar, I., Nallur, S.M., Trang, P., Roush, S., Boehm, M., Gillespie, E., and Slack, F.J. (2007). MicroRNAs as potential agents to alter resistance to cytotoxic anticancer therapy. Cancer Res. *67*, 11111–11116.

Wightman, B., Ha, I., and Ruvkun, G. (1993). Posttranscriptional regulation of the heterochronic gene lin-14 by lin-4 mediates temporal pattern formation in *C. elegans*. Cell *75*, 855–862.

Wightman, B., Bürglin, T.R., Gatto, J., Arasu, P., and Ruvkun, G. (1991). Negative regulatory sequences in the lin-14 3′-untranslated region are necessary to generate a temporal switch during *Caenorhabditis elegans* development. Genes Dev. *5*, 1813–1824.